IL NUOVO CIMENTO **40 C** (2017) 143
DOI 10.1393/ncc/i2017-17143-1

Colloquia: SciNeGHE 2016

Ground-based cosmic ray experiments: A review

A. Castellina
INAF, Osservatorio Astrofisico di Torino and INFN, Sezione di Torino - Torino, Italy

received 3 June 2017

Summary. — A brief overview is given of progress in the knowledge of the cosmic ray origin and nature obtained in recent years by means of ground-based experiments, in the energy region above 10^{14} eV and up to the highest energies. The information obtained from the study of the shape and composition of the primary spectrum are described, with special emphasis on the multi-messenger approach.

1. – Introduction

Cosmic rays are a key ingredient in our understanding of the Universe. In our Galaxy, having an energy density comparable to that of stellar light and magnetic fields, they take part in all chemical processes both in the interstellar medium and in stellar nucleosynthesis. Above about 10^{19} eV they are of extragalactic origin and their spectrum extends to the highest energies, up to 10^{20} eV and above, allowing us to study the acceleration mechanisms in extreme conditions. The long-standing quest for their origin is challenged by their isotropy, although at the highest energies their higher magnetic rigidity could allow for searches of point sources.

Large ground-based experiments constitute the only feasible way to study the cosmic ray origin and properties in the energy range above $\approx 10^{14}$ eV, where the flux of primary particles is too low to allow a direct detection by satellites or balloon-based instrumentation. In ground-based detectors, the energy is measured from the total number of secondary particles detected at the experimental level or by exploiting the emission of Cherenkov light by the shower particles across the atmosphere. At the highest energies, these particles emit fluorescence light in the UV bandwidth, thus allowing for an almost direct, calorimetric measurement of the primary energy. The nature of the primaries is inferred by measuring the different charged components of air showers or the longitudinal profiles in the atmosphere through which their production depths can be determined.

Despite its amazingly regular power-law shape, the energy spectrum of primary cosmic rays shows a few changes of slope, either pointing to a hardening or a softening of the flux, as visible in fig. 1 (where the flux has been multiplied by $E^{2.5}$). These irregularities, complemented by information on the mass composition and the arrival directions of the primary particles, are the key elements to understand the production and propagation of the cosmic ray radiation.

2. – Galactic cosmic rays

The Galactic cosmic rays, most likely accelerated in supernova remnants, form the vast majority of the particles reaching the Earth. Their spectrum is broad, covering energies up to at least few PeV for protons, but there are still open issues related to the maximum energy to which they can be accelerated in the Galactic sources [1].

A steepening (the *"knee"*) in the all-particle spectrum at $\approx 4 \cdot 10^{15}$ eV has been observed by all experiments and in all charged components of the air showers, thus demonstrating its astrophysical origin as opposed to alternative explanations based on possible changes in nucleus-nucleus hadronic interactions (which have also been excluded by the first results from LHC [2]). The difficult task of assigning the origin of the knee to a specific component is still without a final answer: most data suggest it is due to the light component and point to subsequent knees for nuclei at constant rigidity [3]. On the contrary, experiments at high altitude like ARGO and Tibet AS-γ point to a proton knee at much lower energy, around 700 TeV [4, 5]. The analyses are all based on indirect information from extensive air showers, and as such the results are strongly dependent on the models of hadronic interactions employed in the simulations. Furthermore, the experiments do not have the resolution to measure single nuclei, thus making it difficult to compare their results.

A hardening of the spectrum (the *"low energy ankle"*) just above 10^{16} eV and a further steepening at ≈ 0.8–$1 \cdot 10^{17}$ eV (the *"2nd knee"*) are evident in the data from the three main experiments exploring the energy region that covers the end of the Galactic component and the possible onset of the extra-Galactic one: KASCADE-Grande, Tunka and IceTop. Taking into account the differencies in energy resolution and the quoted systematic uncertainties (≈ 20–30%), the three spectra appear to be in quite good agreement. The described features are also seen in the spectrum measured by the low energy extension of Telescope Array ([3] and references therein).

Composition information comes from analyses correlating the muonic and electromagnetic components of the extensive air showers: the steepening at the 2nd knee appears to be associated to the heavy primaries, at an energy ≈ 26 times higher than that of the proton knee, thus confirming the rigidity-dependent cutoff interpretation, as shown in fig. 2.

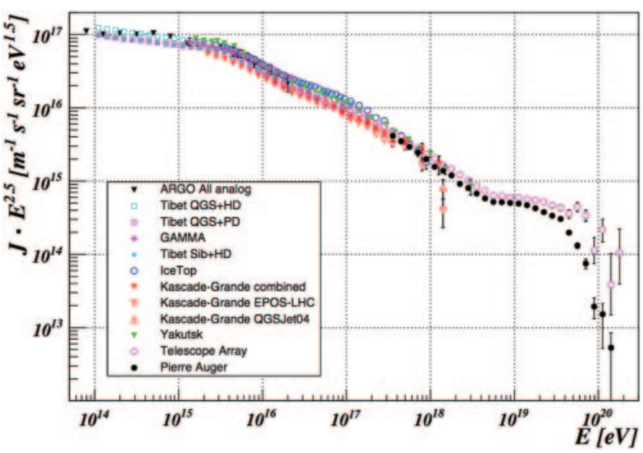

Fig. 1. – Compilation of recent results on cosmic ray energy spectrum (data from [3]).

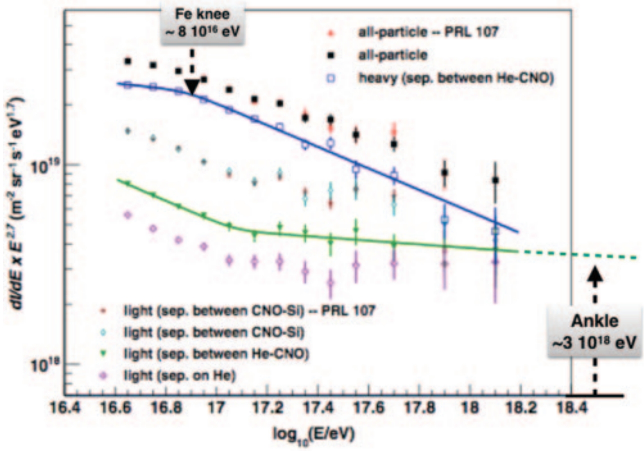

Fig. 2. – Energy spectrum in the transition region for different components (from [6]).

The energy region $[10^{17}$–$10^{19}]$ eV is hosting the transition from a Galactic to an extragalactic origin of the cosmic rays. According to the composition analysis of KASCADE-Grande, the clear hardening in the energy spectrum just above 10^{17} eV pertains to the light component of the primary beam (fig. 2). As such, this feature can be interpreted as the signature of the onset of the extragalactic proton component, thus pointing to an all-particle transition at the *"ankle"*, a hardening of the spectrum at ≈ 4–$5 \cdot 10^{18}$ eV. Some issues appear in the IceTop data, where a too large fraction of iron seems to be present; this can hopefully be solved in the near future when more statistics will be available.

3. – Extragalactic cosmic rays

The ultra high energy region is mainly covered by two experiments: the Pierre Auger Observatory and the Telescope Array. Both employ a hybrid technique: an array of surface detectors (water Cherenkov stations or scintillators respectively) covers a large area overlooked by fluorescence telescopes, able to provide a direct measure of the primary energy and to reconstruct the longitudinal profile of the shower in atmosphere. Note that the quasi-calorimetric energy calibration is not prone to the systematic uncertainties deriving from the limited knowledge of the hadronic interactions.

Both Collaborations clearly measure the ankle at ≈ 4–$5 \cdot 10^{18}$ eV; their fluxes are in good agreement at energies $\leq 2 \cdot 10^{19}$ eV, with differences of about 20%. The suppression of the flux is found in the Auger data with unprecedented significance at $E_s = 42$ EeV, while a higher value of ≈ 56 EeV is claimed by Telescope Array (fig. 3). It is interesting to note that the Telescope Array energy scale would go down by about 14% if the fluorescence yield used in Auger (measured in the AirFly experiment [7]) would be applied.

The mass composition is measured by determining the maximum depth of development of the electromagnetic component of the showers in atmosphere X_{max}. The evolution of the first two moments of the X_{max} distributions in Auger hints to a composition getting lighter from 10^{17} eV to the energy of the ankle, and then getting heavier again above this value. On the contrary, Telescope Array claims a proton-like composition, although their result was shown to be also compatible, within their current systematics,

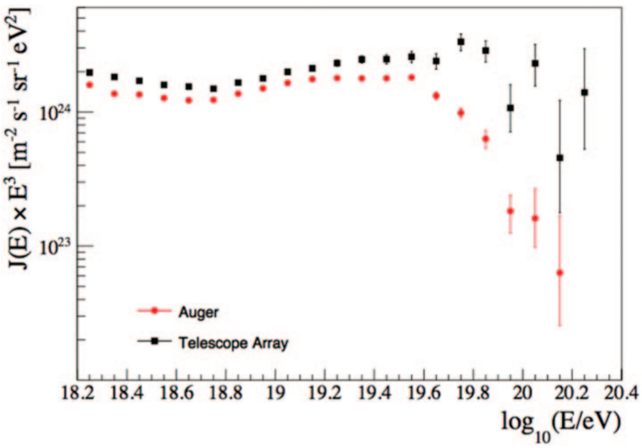

Fig. 3. – The UHE energy spectrum measured by the Pierre Auger and the Telescope Array observatories [3].

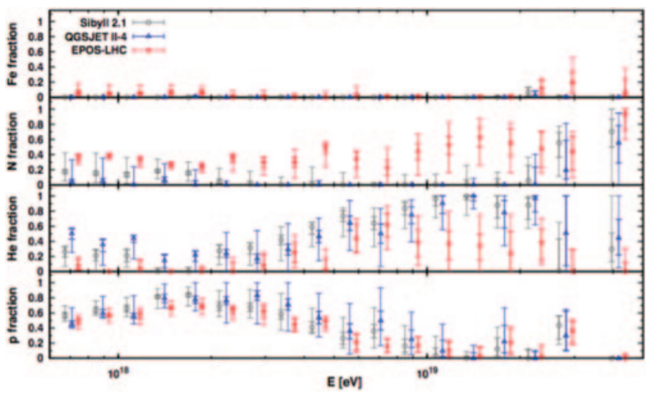

Fig. 4. – Best fitting elemental fractions from a mixture of 4 species as derived from the Pierre Auger data [9].

with an Auger-like, mixed composition [8]. More information come from the study of the whole X_{max} distributions, particularly by Auger thanks to its much larger exposure, ≈ 4 times that of Telescope Array. The data are better reproduced by a mixed composition, while the proton fraction decreases from 60% at the ankle to almost zero at 10^{19} eV. Furthermore, no need for an iron component is required at any energy (fig. 4) [9]. Note that the Pierre Auger data do not show any significant deviation from isotropy within the systematic uncertainties up to the EeV energies, so that protons must be extra-galactic already below $10^{18.5}$ eV. A galactic component would need to be heavy in order not to contribute to any anisotropy.

Both Collaborations provided an astrophysical interpretation from the combined information on spectrum and composition: a fit to simple models of origin and propagation led to different conclusion. In the Auger data, a hard injection spectrum with low rigid-

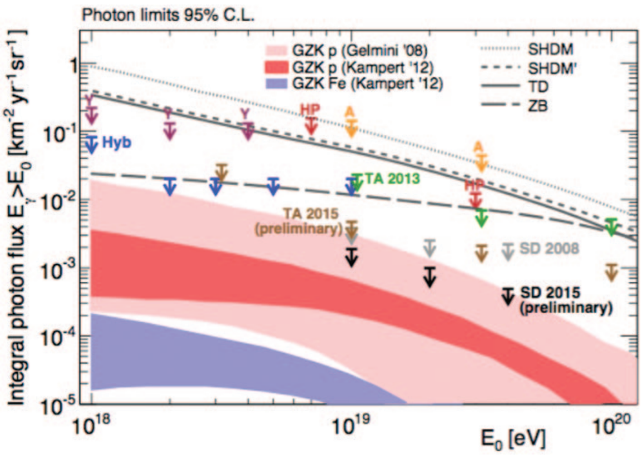

Fig. 5. – Compilation of upper limits to the diffuse photon flux. Expected scenarios from different models and legend from [13].

ity cutoff is favoured, and the suppression is better explained as the energy cutoff of the injection at the sources [10]. For Telescope Array, due to the assumption of a proton-like composition, data appear compatible with a more standard interpretation, where the suppression can be explained as a propagation effect (GZK cutoff) [11].

4. – Multimessengers

A key ingredient in the discrimination among different models of origin and propagation of Galactic and extra-galactic cosmic rays is given by the study of neutral particles: gamma rays, neutrons and neutrinos, having very different travel distances, can be used as probes of either Galactic or extra-Galactic sources, or both.

A diffuse photon flux was searched for in KASCADE-Grande, leading to new upper limits in the range $[2.5 \cdot 10^{14}–1.9 \cdot 10^{16}]$ eV [12]. These limits on γ-rays produced in the TeV to PeV region via the same cosmic ray hadronic interactions responsible for the neutrino emission can be used to set constraints on the Galactic or extra-galactic origin of the IceCube neutrino excess. Note however that most of the IceCube events originate from the Southern hemisphere, a region not constrained by the present limits.

EeV γ and neutron point sources have been searched for in Auger, in both cases leading to exclude Galactic sources, unless transient, or not emitting jets towards Earth, or being too faint ([13] and references therein).

At ultra high energies, a possible detection of cosmogenic photons or neutrinos would provide a direct signature of the GZK cutoff [14]; their fluxes are sensitive to the characteristics of the sources and of the propagation medium used to build plausible astrophysical models. The current limits on the diffuse flux of photons at ultra high energies are shown in fig. 5. The best ones are those derived in the Pierre Auger Observatory, leading to the exclusion of many top-down models, and to the first constraints on the cosmogenic photon fluxes. The most optimistic scenarios of propagation in the hypothesis of proton-only sources were also excluded.

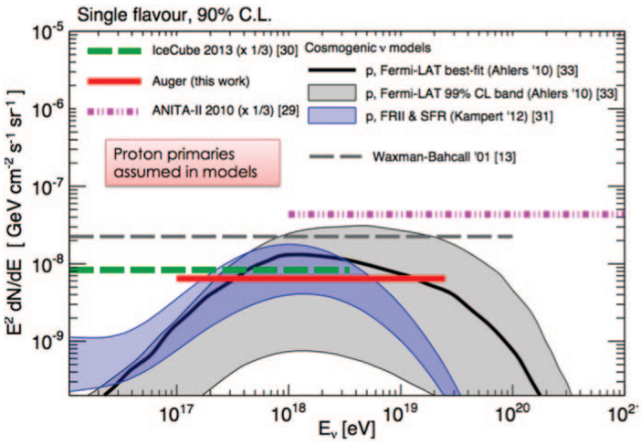

Fig. 6. – 90% CL upper limits to the normalization of the diffuse UHE neutrino flux. Some models are shown for comparison.

Neutrinos can be searched for in the Pierre Auger Observatory; the sensitivity is limited to large zenith angles and energies $\geq 10^{17}$ eV, but it is highest in the energy region where the cosmogenic neutrino flux peaks. As shown in fig. 6, the 90% CL single-flavour limit to the diffuse flux of UHE neutrinos (assuming a differential neutrino flux $\propto E^{-2}$) strongly disfavours models for cosmogenic ν assuming a pure proton composition from sources with strong evolution. In the same figure, models of neutrino production at astrophysical sources as well as the Waxman-Bahcall bound are also shown.

Following the observation of the highest energy neutrinos by IceCube, a joint analysis was set up to search for correlations among the neutrino candidates and the UHE cosmic rays measured by the Pierre Auger Observatory and the Telescope Array [15]. Although no significant hints for correlation were seen, the excesses found arise from pairs of events from the regions of the sky corresponding to the largest excesses observed by Telescope Array (the *"hot spot"* [16]) and Pierre Auger (near the super-Galactic plane).

A final example of multi-messenger searches is given by the UHE neutrino follow-up of the gravitational-wave (GW) events detected by Advanced LIGO. The inferred source, *i.e.* the coalescence of a stellar mass binary black hole sytem can in principle provide an environment for the production of UHE cosmic rays, γ and neutrinos. No UHE neutrino candidates were found in Auger, leading to the first limit from extensive air showers on the (declination dependent) radiated energy in neutrinos at $E > 10^{17}$ eV [17].

5. – Future prospects

Future projects and upgrades of existing detectors demonstrate the vitality of the field. Further and more precise information about the knee region will be obtained by the new hybrid Tibet experiment and by the large LLHASO observatory in China. The transition region will take advantage from the new data of IceTop-2, which will extend the current IceTop to about 10 km^2 area.

At the highest energy, both upgrades of Telescope Array and Auger are currently under deployment. The former will enhance the area by a factor ≈ 4, similar to the current Auger one. The latter aims at a better measure of the primary composition by exploiting scintillator detectors on top the water Cherenkov stations ([3] and references therein), thus extending it to the suppression region. Together with a more and more productive Collaboration among the different groups, by means of joint analyses and multi-messenger studies, many of the currently open questions will be addressed and answered.

REFERENCES

[1] Blasi P., *C. R. Phys.*, **15** (2014) 329.
[2] Ostapchenko S., *Prog. Theor. Phys. Suppl.*, **193** (2012) 204.
[3] Verzi V., *Pos* **(ICRC2015)**, (2016) 15.
[4] Argo Collaboration (Bartoli B. *et al.*), *Phys. Rev. D*, **91** (2015) 112017.
[5] Tibet AS-γ Collaboration (Huang J. *et al.*), *Pos* **(ICRC2015)**, (2016) 421.
[6] Kascade-Grande Collaboration (Apel W. D. *et al.*), *Astropart. Phys.*, **47** (2013) 54.
[7] Ave M. *et al.*, *Astropart. Phys.*, **42** (2013) 90.
[8] Unger M. for the Pierre Auger and the Telescope Array Collaborations, *PoS*, **ICRC2015** (2016) 307.
[9] Pierre Auger Collaboration (Aab A. *et al.*), *Phys. Rev. D*, **90** (2014) 122006.
[10] Pierre Auger Collaboration (Aab A. *et al.*), arXiv:1612.07155 (2017).
[11] Telescope Array Collaboration (Kido E. *et al.*), *Pos* **(ICRC2015)**, (2016) 528.
[12] Kascade-Grande Collaboration (Feng Z. *et al.*), *Pos* **(ICRC2015)**, (2016) 823.
[13] Pierre Auger Collaboration (Aab A. *et al.*), *Astrophys. J. Lett.*, **837** (2017) L25.
[14] Settimo M. and de Domenico M., *Astropart. Phys.*, **62** (2015) 92.
[15] The IceCube, Pierre Auger and Telescope Array Collaboration, *J. Cosmol. Astropart. Phys.*, **01** (2016) 037.
[16] Telescope Array Collaboration (Abbasi R. U. *et al.*), *Astrophys. J. Lett.*, **790** (2014) L21.
[17] Pierre Auger Collaboration (Aab A. *et al.*), *Phys. Rev. D*, **94** (2016) 122007.